Smart Structures and Systems, Vol. 3, No. 3 (2007) 263-280
DOI: http://dx.doi.org/10.12989/sss.2007.3.3.263

Vibration-based damage detection in beams using genetic algorithm

Jeong-Tae Kim† and Jae-Hyung Park‡

Department of Ocean Engineering, Pukyong National University, Busan, Korea

Han-Sam Yoon‡†

Research Center for Ocean Industrial Development, Pukyong National University, Busan, Korea

Jin-Hak Yi‡‡

Korea Ocean Research & Development Institute, Ansan, Korea

(Received August 1, 2006, Accepted October 25, 2006)

Abstract. In this paper, an improved GA-based damage detection algorithm using a set of combined modal features is proposed. Firstly, a new GA-based damage detection algorithm is formulated for beam-type structures. A schematic of the GA-based damage detection algorithm is designed and objective functions using several modal features are selected for the algorithm. Secondly, experimental modal tests are performed on free-free beams. Modal features such as natural frequency, mode shape, and modal strain energy are experimentally measured before and after damage in the test beams. Finally, damage detection exercises are performed on the test beam to evaluate the feasibility of the proposed method. Experimental results show that the damage detection is the most accurate when frequency changes combined with modal strain-energy changes are used as the modal features for the proposed method.

Keywords: genetic algorithm; damage detection; vibration-based; natural frequency; modal strain-energy; free-free beam.

1. Introduction

During the past several decades, a significant amount of research has been conducted in the area of nondestructive damage detection via changes in modal responses of a structure. These methods utilize modal features such as natural frequency, frequency response function, mode shape, and modal strain energy (Kim 2001, Sohn, *et al*. 2003). Research efforts have been mainly focused on developing

†Professor, Corresponding Author, E-mail: idis@pknu.ac.kr
‡Research Assistant
‡†Assistant Professor
‡‡Senior Research Scientist

appropriate techniques of sensing and monitoring, damage identification, and performance evaluation of damaged structures. Research works on damage detection techniques include Kalman filter method (Hoshiya and Saito 1984), modal strain energy-based damage index (DI) method (Stubbs, *et al*. 2000, Kim, *et al*. 2003a), genetic algorithm (GA)-based method (Mares and Surace, 1996, Chou and Ghaboussi 2001, Raich and Liszkai 2003, Rao, *et al*. 2004), and artificial neural network (ANN)-based method (Wu, *et al*. 1992, Choi and Kwon 2000). Among those, the GA-based damage detection methods have been studied to locate and assess structural damages via system identification (SID) using genetic optimization process. Compared to the other optimization methods, the GA-based methods do not need any differential information on objective functions. Also, the accuracy of damage detection can be improved by statistical multi-points-search algorithm (Goldberg 1999).

There exist several problems that should be overcome to develop a rigorous GA-based damage detection method. First, the computation process of the GA-based method requires relatively longer time-consumption for damage detection compared to other methods (i.e. DI method or ANN method). Second, its accuracy depends on the types of modal features that are selected for the damage detection. Third, a baseline model should be created by an appropriate system identification process. The inaccuracy of the baseline model leads to faults in damage detection. There have been several research attempts in order to overcome the problems. Au, *et al*. (2003) proposed methods using a micro genetic algorithm that reduces the calculation time. Routolo and Surace (1997) improved the accuracy of GA-based damage detection by using an objective function combined modal features such as natural frequencies, mode shapes, and mode curvatures. To reduce the effect of modeling error, Hao and Xia (2002) also proposed a GA-algorithm using the changes of natural frequencies and mode shapes between pristine and damaged states. In spite of those research efforts, however, the following research needs remain to improve the accuracy of GA-based damage detection. First, a robust GA-algorithm should be developed to reduce the effect of model errors on damage detection process. Second, a set of modal features representing structural characteristics should be selected to discriminate damaged states from undamaged pristine state. Maia, *et al*. (2003) and Kim, *et al*. (2003a) studied on the performance of modal features (such as natural frequency, mode shape, mode curvature, and modal strain energy) for the damage detection accuracy in structures. They concluded that modal strain energy is more sensitive to damages in the structures (e.g. beam and truss) than any other modal features.

In this study, an improved GA-based damage detection algorithm using a set of combined modal features that include natural frequency, mode shape, and modal strain energy is proposed. In order to achieve the objective, the following approaches are implemented. Firstly, a new GA-based damage detection algorithm is formulated for beam-type structures. A schematic of the GA-based damage detection algorithm is designed and objective functions using a set of modal features are selected for the algorithm. Modal features selected for the algorithm include frequency changes, mode-shape changes, modal strain-energy changes, frequency changes combined with mode-shape changes, and frequency changes combined with modal strain-energy changes. Secondly, experimental modal tests are performed on free-free beams. Sensor locations are determined from the numerical analyses. Modal features such as natural frequency, mode shape, and modal strain energy are experimentally measured before and after damage in the test beams. Finally, damage detection exercises are performed on the test beams to verify the feasibility of the proposed method.

2. GA-based damage detection technique

2.1. GA-based damage detection algorithm

Structural damage is typically related to change in the structural physical parameters. In damage detection, damage is usually represented by an elemental stiffness reduction factor (SRF) in order to preserve the structural connectivity and reduce the unknown variables. The SRF is defined as the ratio of the elemental stiffness reduction to the initial stiffness. It ranges from 0 to 1, where 0 signifies no damage in the element and 1 means that the element loses its stiffness completely. The objective of damage detection is to derive the SRFs by which nonzero terms locate the damage and their magnitudes represent the damage severities (Hao and Xia 2002).

In GA-based damage detection techniques, structural damage is estimated from model update process using damage-induced changes in modal features. As shown Fig. 1, an analytical model is continuously updated until the difference between experimental and analytical modal features is minimized. This process is defined as the minimization problem and it can be formulated as follows:

$$\begin{aligned} &\text{Find } \alpha \\ &\text{Minimize } J(\alpha) = [A - B(\alpha)]^2 \\ &\text{Subject to } g(\alpha) < 0,\ h(\alpha) = 0 \end{aligned} \tag{1}$$

where α is element's SRF vector, $J(\alpha)$ is objective function for damage detection, A is experimental modal feature extracted from the target structure, $B(\alpha)$ is analytical modal feature calculated from the analytical model of the test structure, and $g(\alpha)$ and $h(\alpha)$ are equality and inequality constraints, respectively. In this study, $g(\alpha)$ and $h(\alpha)$ are not used for damage detection. In GA-based damage assessment, the accuracy of damage detection depends on the feasibility of modal features and a baseline analytical model that are selected for the test structure (Routolo and Surace 1997, Lee and Yun 2006). Also, the time consumed for damage detection process would be reduced by using optimization techniques (Routolo and Surace 1997, Au, *et al*. 2003).

In this study, micro GA is applied to minimize Eq. (1). Traditional genetic algorithms use large population to keep up the variety of genetic information; however, micro GA uses very small population that makes it efficient for searching optimum solution (Au, *et al.* 2003). Fig. 2 schematizes the damage detection process using the micro GA. Firstly, five (5) individuals, which represents stiffness reduction factors, are initialized randomly in a population. Then the fitness that represents the maximized level of objective function is evaluated for each individual. Secondly, if all individuals are converged to a point,

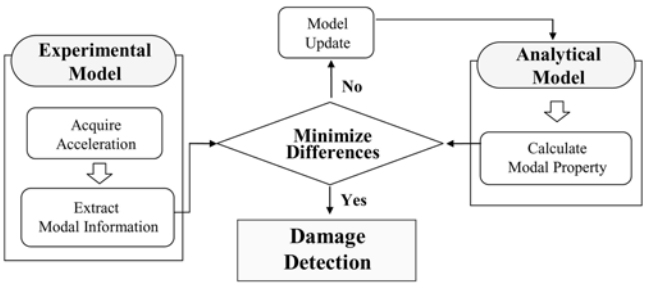

Fig. 1 GA-based damage detection process

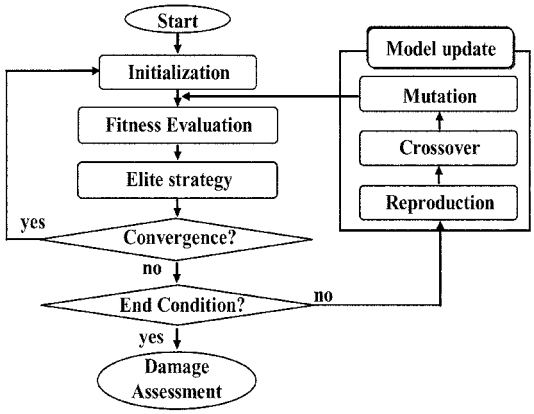

Fig. 2 Schematic of micro GA-based damage detection algorithm

they are restarted and initialized. If they are not converged to a point and do not satisfy the end condition, they are updated by genetic operators such as reproduction, crossover, and mutation. The algorithm uses elite strategy that reintroduces the best individual from the previous generation in the present generation when the best individual from the previous generation is lost in the present generation. These processes are repeated until the end condition is satisfied and the damages are assessed from the optimized analytical model.

2.2. Theoretical background of modal features

Consider an Euler-Bernoulli beam system of NE elements (j = 1,2,..., NE) and a measured set of NM vibration modes (i = 1,2,..., NM). The system yields the ith natural frequency ω_i and ith mode shape ϕ_i. The ith modal strain energy of the pristine state can be written as follows (Kim, *et al.* 2003a):

$$U_i = \int_0^L \frac{1}{2} k(x)[\phi_i''(x)]^2 dx \tag{2}$$

where, U_i is the ith modal strain energy, $k(x)$ is flexural stiffness of the beam, L is the beam's span length, and $\phi_i''(x)$ is the ith modal curvature that can be determined from the ith mode shape. Assuming that the stiffness is constant in the jth element, then the ith modal strain energy allocated in the jth element (between x_k and x_{k+1}) is given by:

$$U_{ij} = \frac{1}{2} k_j \int_{x_k}^{x_{k+1}} [\phi_i''(x)]^2 dx \tag{3}$$

By dividing L.H.S. of Eq. (3) by the unknown element stiffness of the undamaged jth element (k_j), the modal strain energy can be written in terms of measurable modal curvature function as follows:

$$2U_{ij}/k_j = \int_{x_k}^{x_{k+1}} [\phi_i''(x)]^2 dx \tag{4}$$

where U_{ij} is the pre-damaged modal strain energy for the ith mode and the jth element. By expanding Eq. (4) into all NE elements, the relative modal strain energy of the ith mode of the undamaged state can be defined as follows:

$$\theta_i = 2\sum_{j=1}^{NE} U_{ij} / k_j = \sum_{j=1}^{NE} \int_{x_k}^{x_{k+1}} [\phi_i''(x)]^2 dx \tag{5}$$

Next, assume that at some later time the structure is damaged (e.g. stiffness loss) in one or more locations of the structure. The resulting characteristic equation of the damaged structure yields ω_i^* and ϕ_i^*. Note that the asterisk denotes the damaged state. Then the relative modal strain energy of the i^{th} mode of the damaged state can be written as follows:

$$\theta_i^* = 2\sum_{j=1}^{NE} U_{ij}^* / k_j^* = \sum_{j=1}^{NE} \int_{x_k}^{x_{k+1}} [\phi_i''^*(x)]^2 dx \tag{6}$$

where U_{ij}^* is the post-damaged modal strain energy for the ith mode and jth element, k_j^* is the unknown element stiffness of the damaged jth element.

2.3. Objective function using single modal feature

2.3.1. Frequency changes

An objective function is formulated in terms of fractional changes in natural frequencies for the structures before and after damage. It is used to reduce the effect of modeling errors as follows (Hao and Xia 2002, and Lee and Yun 2006):

$$F_\omega(\alpha) = \sum_{i=1}^{NM} \left(\frac{\delta^E \omega_i}{{}^E\omega_i} - \frac{\delta^A \omega_i(\alpha)}{{}^A\omega_i} \right)^2 \tag{7}$$

where ${}^E\omega_i$ and ${}^A\omega_i$ are experimental natural frequency and analytical natural frequency of the ith mode for pristine state, respectively. Also, $\delta^E\omega_i$ and $\delta^A\omega_i$ are fractional changes of the experimental natural frequency and that of the analytical natural frequency, respectively. An analytical model should be modeled to represent the baseline, pristine state of the target structure. Then the stiffness reduction factor α of the analytical model is updated until the fractional changes of the analytical natural frequencies in the pre- and post-damaged state become converged to those of the experimental natural frequencies in the pre- and post-damaged state.

2.3.2. Mode-shape changes

The primary disadvantages of methods using only the fractional change of natural frequencies are as follows: natural frequency is not sensitive enough to local damage; and damages in symmetric locations may not be distinguished (Routolo and Surace 1997, Hao and Xia 2002). If mode shapes are measured at N points, an objective function using mode shapes is written as follows:

$$F_\phi(\alpha) = \sum_{i=1}^{NM} \sum_{j=1}^{N} ([{}^A\phi_{ij} - {}^A\phi_{ij}^*(\alpha)] - [{}^E\phi_{ij} - {}^E\phi_{ij}^*])^2 \tag{8}$$

where ${}^A\phi_{ij}$ and ${}^E\phi_{ij}$ are analytical mode shape and experimental mode shape for ith mode and jth point of the undamaged state. The asterisk denotes post-damage state. The objective function using the mode shape is utilized to evaluate the performance of damage detection of the proposed technique.

2.3.3. Modal strain-energy changes

The primary disadvantages of methods using modal parameters are as follows: modal parameters are not sensitive to small local damage; and environmental effect on modal parameters leads to false detection of damage (Kim, *et al.* 2003b). In order to overcome these problems, alternative objective functions are needed. An objective function using changes in modal strain energies before and after structural damage is defined as follows:

$$F_\theta(\alpha) = \sum_{i=1}^{NM}\sum_{j=1}^{N}([{}^A\theta_{ij} - {}^A\theta^*_{ij}(\alpha)] - [{}^E\theta_{ij} - {}^E\theta^*_{ij}])^2 \tag{9}$$

where ${}^A\theta_{ij}$ and ${}^E\theta_{ij}$ are analytical modal strain energy and experimental modal strain energy for ith mode and jth element of the undamaged state. The asterisk denotes post-damage state.

2.4. Objective function using multiple modal features

2.4.1. Frequency changes combined with mode-shape changes

From the minimization process of two objective functions (i.e. Eq. (7) and Eq. (8)), damage can be indicated as optimal design values (e.g. stiffness reduction factors) (Hao and Xia 2002). By treating as the single objective optimization problem, the two objective functions are linearly combined using weight values as follows:

$$J_1(\alpha) = W_\omega F_\omega(\alpha) + W_\phi F_\phi(\alpha) \tag{10}$$

where W_ω is the weight for $F_\omega(\alpha)$ (i.e., the objective function using natural frequency) and W_ϕ is the weight for $F_\phi(\alpha)$ (i.e. the objective function using mode shape). Since the genetic algorithm needs a process to solve maximization problems, Eq. (10) is converted to the following form of the maximization problem:

$$\overline{J}_1(\alpha) = \gamma_1 - J_1(\alpha) \tag{11}$$

where γ_1 is arbitrary constant that always makes $J_1(\alpha)$ positive real number. In this study, γ_1 was used to 100. The weights are empirically determined. The weight for natural frequency is usually larger than the weights for other modal properties (Friswell, *et al.* 1998).

2.4.2. Frequency changes combined with modal strain-energy

From the minimization process of the two objective functions (i.e. Eq. (7) and Eq. (9)), damage can be indicated as optimal design values (e.g. stiffness reduction factors). By treating as the single objective optimization problem, the two objective functions are linearly combined using weight values as follows:

$$J_2(\alpha) = W_\omega F_\omega(\alpha) + W_\theta F_\theta(\alpha) \tag{12}$$

where W_ω is the weight for $F_\omega(\alpha)$ and W_θ is the weight for $F_\theta(\alpha)$ (i.e., the objective function using modal strain energy). Further, Eq. (12) is converted to the following form:

$$\overline{J}_2(\alpha) = \gamma_2 - J_2(\alpha) \tag{13}$$

where γ_2 is an arbitrary constant that keeps $J_2(\alpha)$ positive real number. In this study, γ_2 was used to 100.

3. Experimental modal test

3.1. Description of test structure

For the verification of proposed technique, experimental tests were performed on free-free beams. The free-free beam was selected to reduce modeling uncertainty related to support boundary conditions. As shown in Fig. 3, the dimensions of the test beam are as follows: span length (L) 55.8 cm, width (B) 4 cm, and thickness (t) 1 cm. The material of the test beam is aluminum and its elastic modulus is 70 GPa and linear mass density is 2,700 kg/m^3. The test beam was hanged by using two thin nylon strings at 2 cm inside from both edges.

3.2. Verification of sensor locations

In order to verify the number of sensors required for the proposed damage detection method, numerical tests were performed on an analytical model of the test structure. For damage detection, at least a few natural frequencies and mode shapes should be measured and modal strain energies corresponding to the measured modes should be computed. In most mode-shape-based damage detection methods, those needs should be satisfied by utilizing enough sensors because the amount of modal data is directly related to the performance of the damage detection methods.

As the analytical model, we used the Euler-Bernoulli beam model with 13 nodes and 12 elements as shown in Fig. 4. For sensor locations, two cases were considered: (1) Sensor Layout 1: 13 sensors corresponding to all 13 nodes; and (2) Sensor Layout 2: 7 sensors corresponding to 7 odd nodes (i.e., 1, 3, 5,..., 13). Note that 7 sensor locations are the least sensors that should be arranged to extract the four bending mode shapes. Natural frequencies and mode shapes of the first four modes were obtained from numerical modal analyses, as listed in Table 1 and also shown in Fig. 5. Damages were inflicted to Element 6 and 12 by simulating 30% reduction of flexural stiffness, as shown in Fig. 6. Natural frequencies of the damaged state were listed in Table 1.

To verify the performance of the selected sensors, we examined the accuracy of damage detection by the proposed method using the frequency changes combined with the modal strain-energy changes, as

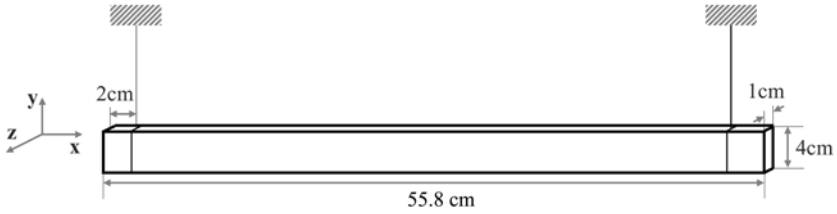

Fig. 3 Description of test structure

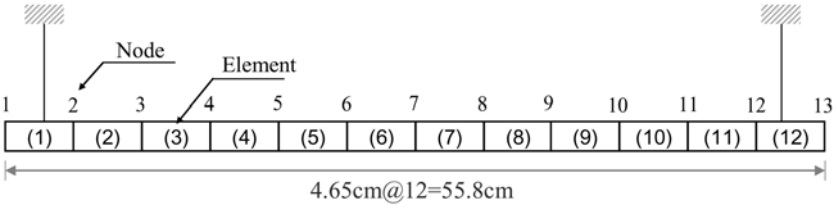

Fig. 4 Analytical model of free-free beam

Table 1 Natural frequencies of analytical model

Damage Scenario	Natural Frequency (Hz)			
	Mode 1	Mode 2	Mode 3	Mode 4
Undamaged	166.90	460.12	902.31	1492.7
30% Stiffness Reduction in Elements 6 & 12	160.08	457.76	879.50	1471.2

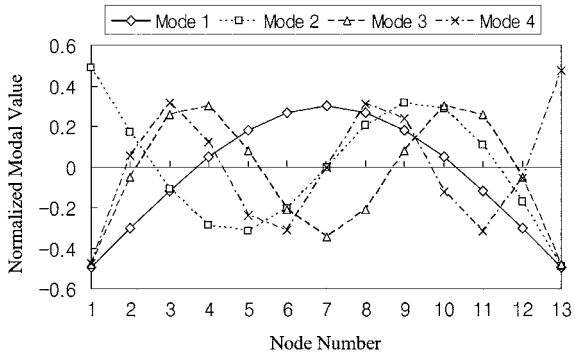

Fig. 5 Mode shapes calculated in undamaged state

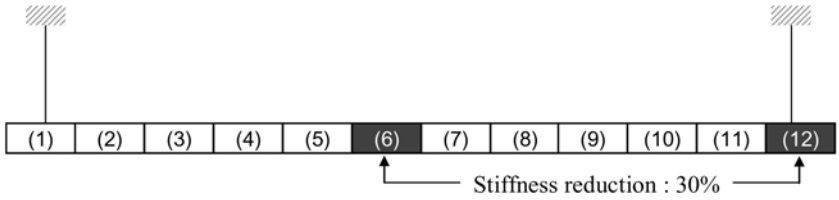

Fig. 6 Inflicted damage locations and severities in analytical model

described in Eq. (12). Damage detection using the proposed micro GA approach was performed as follows. Firstly, 4,000 generations was selected for the algorithm's end condition which is needed to search the global optimum. Secondly, each design variable consisted of 13 bits, for which each variable range 0.1809~1.0 and the resolution is 10^{-4}. Thirdly, the genetic operators were selected as tournament selection, one-point crossover and simple mutation. Fourthly, the elite strategy was implemented to prevent the loss of the best individual from the previous generation. The parameters used in the genetic algorithm are as follows: the population size is 5; the probability of crossover is 1.0; and the probability

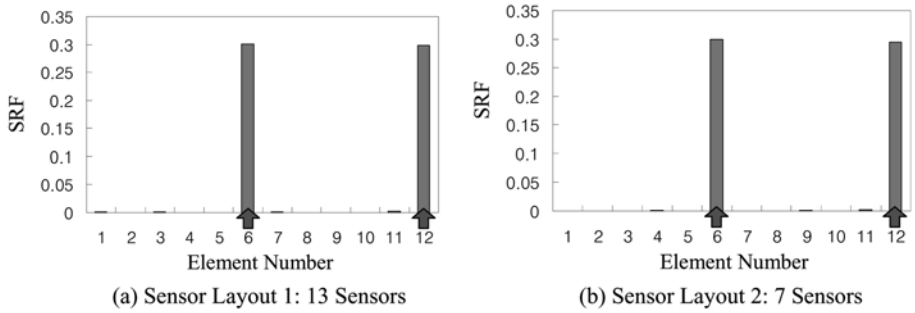

Fig. 7 Damage detection results for analytical model

of mutation is 0.02. The results of damage detection are shown in Fig. 7. Both Sensor Layout 1 (13 accelerometers) and Sensor Layout 2 (7 accelerometers) produce the accurate localization and severity estimation of the inflicted damages at Element 6 and Element 12. It seems that the use of 7 sensors is enough for implementing the proposed method with frequency and mode-shape information to the target beam.

3.3. Experimental setup

As shown in Fig. 8 and Fig. 9, seven sensors were placed on the test beam at uniform intervals and impact force was applied at x/L=0.108 from the left edge. The data acquisition system includes Dytran 3101BG miniature accelerometers, NI-PXI-4472 data acquisition board, and a PC with LabVIEW software. As shown in Fig. 10, acceleration signals were acquired for a second by setting sampling rate of 8000 Hz. Natural frequencies and mode shapes of the first four modes were extracted from the measured acceleration signals by using the frequency domain decomposition (FDD) technique (Yi and Yun, 2004).

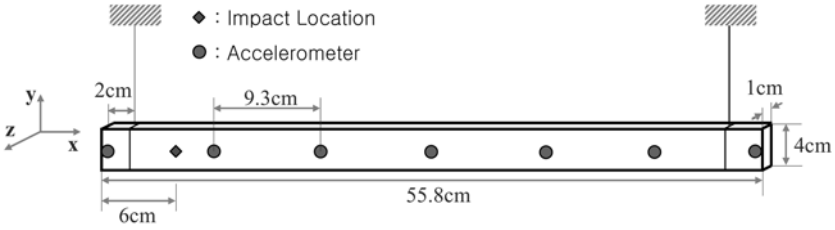

Fig. 8 Accelerometers and impact locations in free-free beam

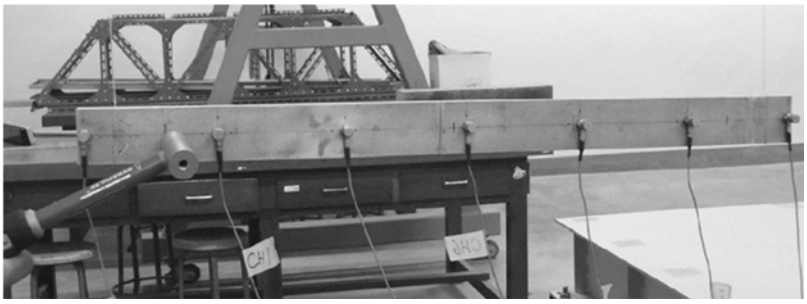

Fig. 9 Test layout of free-free beam

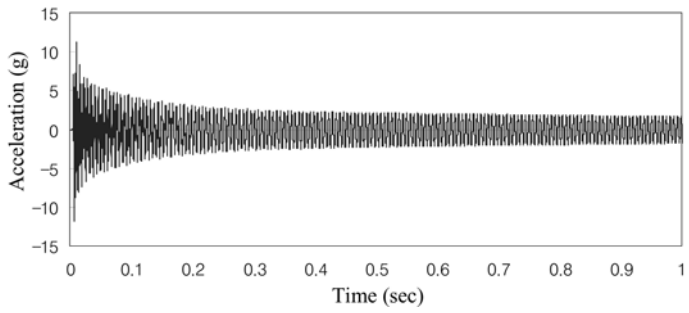

Fig. 10 Acceleration signals of Sensor 4 measured from impact hammer test

Table 2 Pre-damage frequencies for experimental test and analytical model

Test Case	Natural Frequency (Hz)			
	Mode 1	Mode 2	Mode 3	Mode 3
Experimental Test	165.039	452.148	880.859	1445.31
Analytical Model	166.900	460.110	902.271	1492.52

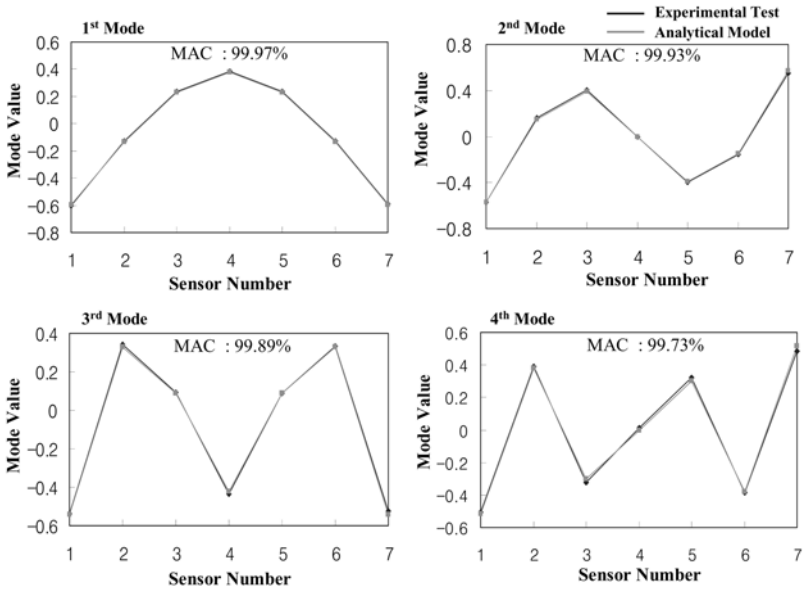

Fig. 11 Mode shapes of experimental test and analytical model in undamaged states

Table 2 and Fig. 11 show the experimental natural frequencies and mode shapes measured from the test beam. Those experimental modal parameters are compared to the analytical results from the numerical analyses described in the previous section (e.g. Table 1 and Fig. 5). There exist differences between the analytical and experimental modal parameters, which may be due to modeling and measurement errors. Note that the fractional changes in modal parameters between before and after damage are utilized for the objective functions, as described previously, to minimize the effect of those errors in the modal parameters on the damage detection accuracy (Kim and Stubbs 1995, Hao and Xia 2002, Lee and Yun 2006).

We selected four damage scenarios as listed in Table 3 and depicted in Fig. 12. Two bending cracks were inflicted at a point near the center (x/L = 0.466) and another near the right edge (x/L = 0.935). Also, two levels of damage-sizes were introduced by sawing off 25% (a/t = 0.25) and 50% (a/t = 0.5) of the

Table 3 Damage scenario of experimental tests

Damage Case	Damage Location (x/L)	Damage Size (a/t)
1	0.466	0.25
2	0.466	0.5
3	0.466, 0.935	0.5, 0.25
4	0.466, 0.935	0.5, 0.5

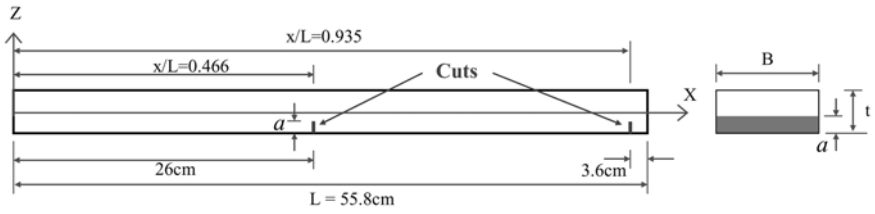

(a) Damage Locations

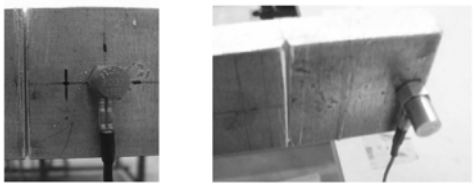

(b) Sawed Cuts

Fig. 12 Damage locations and sawed cuts

Table 4 Natural frequencies measured from experimental tests

Damage Case	Natural Frequency (Hz)			
	Mode 1	Mode 2	Mode 3	Mode 4
Reference	165.039	452.148	880.859	1445.31
1	163.086	451.172	873.047	1442.38
2	158.203	451.172	856.445	1436.53
3	158.203	450.195	855.469	1432.62
4	158.203	450.195	851.563	1416.02

beam thickness (t), respectively. As listed in Table 4, post-damage natural frequencies of the first four modes were measured from the impact hammer tests.

4. Damage detection in test beam

Four damage cases are applied to evaluate the presented 5 methods described in Eq. (7)-Eq. (13). Using the proposed micro GA, each objective function (i.e. Eq. (7)-(10) and (12)) is minimized to detect damages. The micro GA was performed in the following manners. Firstly, 10,000 generations was selected for the algorithm's end condition which is needed to search a global optimum. Secondly, each design variable consisted of 13 bits, for which each variable range 0.1809~1.0 and the resolution is 10^{-4}. Thirdly, the genetic operators were selected as tournament selection, one-point crossover and simple mutation. Fourthly, the elite strategy was implemented to prevent the loss of the best individual from the previous generation. The parameters used in the genetic algorithm are as follows: the population size is 5; the probability of crossover is 1.0; and the probability of mutation is 0.02. To discriminate the global optimum from local optimums, we set a decision rule such that any optimum indication belongs to the global optimum if the indication is sequentially repeated four times.

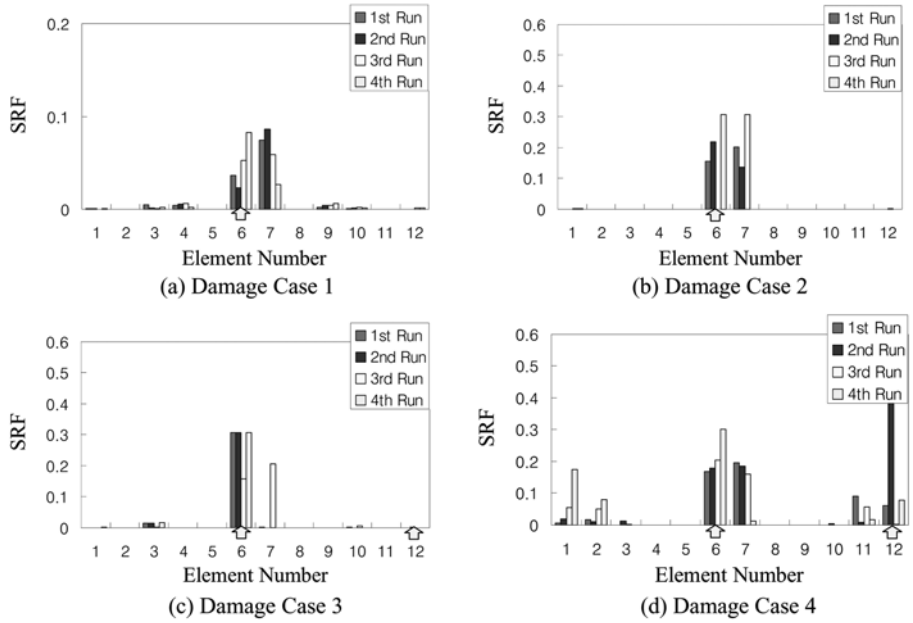

Fig. 13 Damage detection results with frequency changes

4.1. Damage localization

4.1.1. Damage localization with frequency changes

The four measured natural frequencies of pre- and post-damage states are used to predict locations and severities of damage. By using the proposed micro GA, Eq. (7) is minimized for each damage case. Damage detection results are shown in Fig. 13. Note that the two actual damages (one near the mid-span and the other near the right edge) are corresponding to Elements 6 and 12. From the figure, elements' SRFs do not converge to the real damage locations for all damage cases. This is due to symmetric behaviors of the structure which cannot be differentiated in the natural frequencies.

In Damage Cases 1 and 2, the damage inflicted near the mid-span (i.e. Element 6) was detected correctly. In Damage Cases 3, Element 6 was detected but Element 12 was not detected. In Damage Case 4, Element 6 was detected and Element 12 was detected except the 3rd run. In all damage cases, extra locations were falsely predicted due to the symmetric behaviors of the test beam (Note that Elements 1 and 7 are symmetric to Elements 12 and 6). From these results, it is analyzed that the frequency data alone are not sufficient for accurate damage detection in the test structure.

4.1.2. Damage localization with mode-shape changes

By using the four measured mode shapes of pre- and post-damage states, Eq. (8) is minimized to detect the damages. The damage detection results are shown in Fig. 14. For all four damage cases, all 12 elements of the test beam were indicated as being damaged, which are false predictions. This problem may be caused by the existence of many local optimums. Usually, most global optimization methods including GA show the difficulty in searching the global optimum when there are too many local optimums.

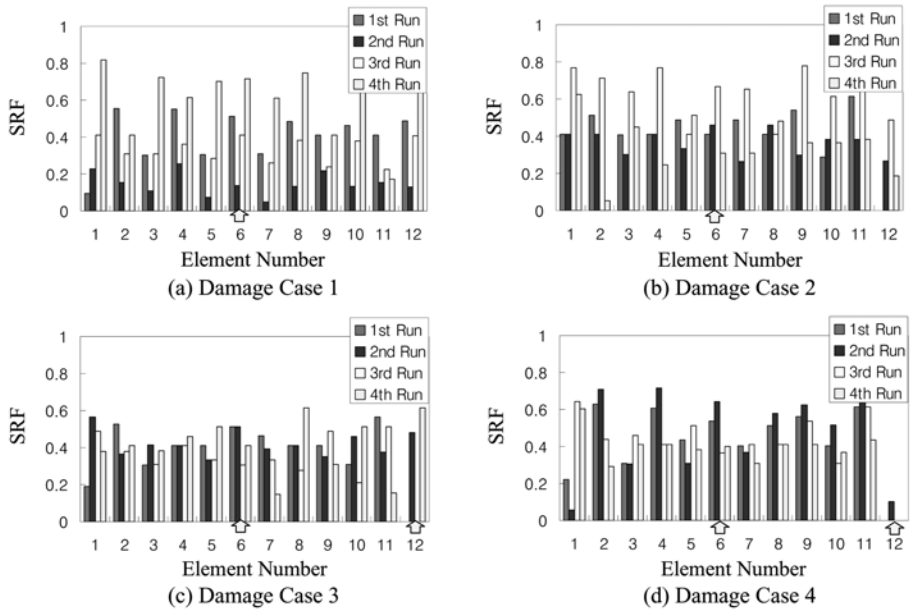

Fig. 14 Damage detection results with mode-shape changes

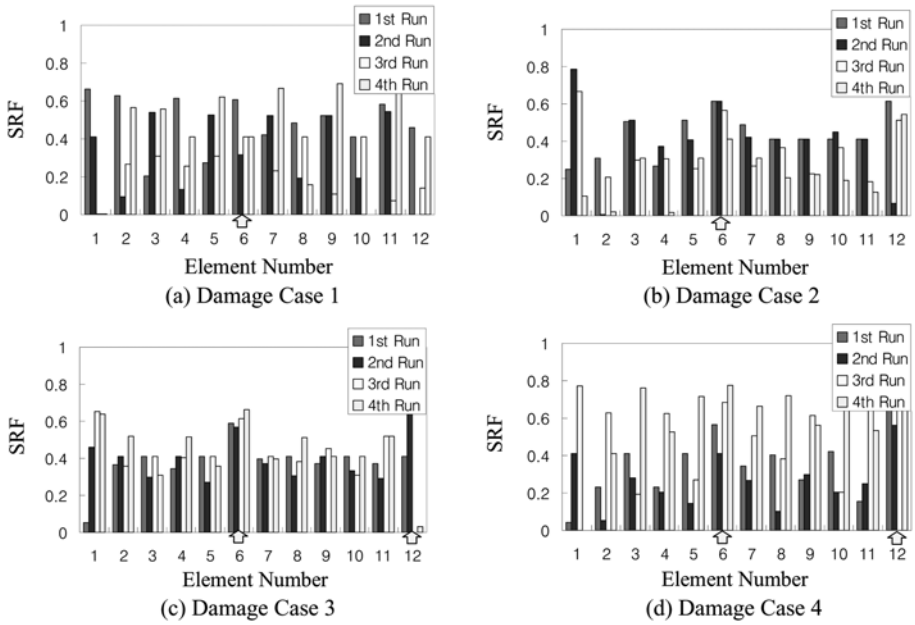

Fig. 15 Damage detection results with modal strain-energy changes

4.1.3. Damage localization with modal strain-energy changes

By using the four measured modal strain-energies of pre- and post-damage states, Eq. (9) is minimized to detect damages. The damage detection results are shown in Fig. 15. For all four damage cases, all 12 elements of the test beam were indicated as being damaged, which are similar false predictions as the previous case.

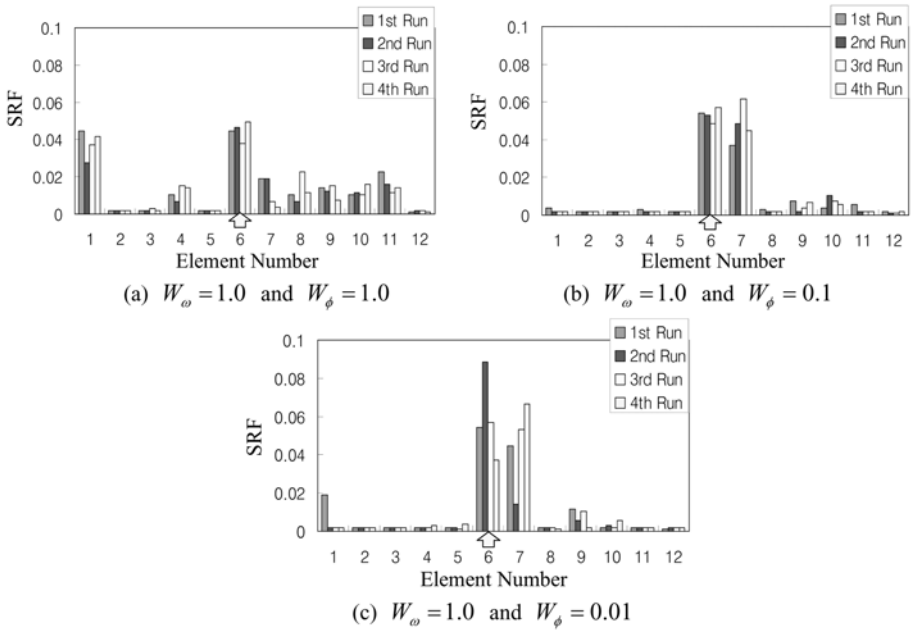

Fig. 16 Damage detection results to decide optimal weights for natural frequency and mode-shape (Damage Case 1)

4.1.4. Damage localization with both frequency changes and mode-shape changes

With the 4 measured frequencies and mode-shapes before and after damages, Eq. (10) is minimized to detect damages. Considering the relative contribution of the frequencies and the mode-shapes to the objective function, W_ω is taken as unity and W_ϕ is taken as 1.0, 0.1 and 0.01, respectively. To decide the best weight for the mode shape, Damage Case 1 was tested as follows. Firstly, when W_ϕ is 1.0, the damage detection results as shown in Fig. 16(a) tend to be similar to those with the mode-shape changes only as shown in Fig. 14(a). Secondly, when the weights are 0.1 and 0.01, the damaged elements are correctly detected as shown in Figs. 16(b) and 16(c).

We selected the weight of 0.1 as the best weight for the mode shape. With the selected the best weight, consistent results were predicted in subsequent four runs of GA processes. In all damage cases, Element 6 was predicted correctly but Element 12 was not detected, as shown in Fig. 17. Also, extra locations were falsely predicted due to the symmetric behaviors of the test beam (Note that Element 7 is symmetric to Element 6). It is observed that the damage detection results using the natural frequency and the mode shape are similar to those with the frequency changes only, as shown in Fig. 13.

4.1.5. Damage localization with both frequency changes and modal strain-energy changes

With the 4 measured frequencies and modal strain-energies before and after damages, Eq. (12) is minimized to detect damages. Considering the relative contribution of the frequencies and the modal strain-energies to the objective function, W_ω is taken as unity and W_θ is taken as 1.0, 0.1 and 0.01, respectively. To decide the optimum weight for the modal strain-energy, Damage Case 1 was tested as follows. Firstly, when W_θ is 1.0, the damage detection results as shown in Fig. 18(a) tend to be similar to those with modal strain-energy changes only as shown Fig. 15(a). Secondly, when the weight is 0.1, the damaged elements are correctly detected and there is false detection for Element 12, as shown in Fig. 18(b). Thirdly, when the weight decrease to 0.01, the influence of modal strain energies are nearly

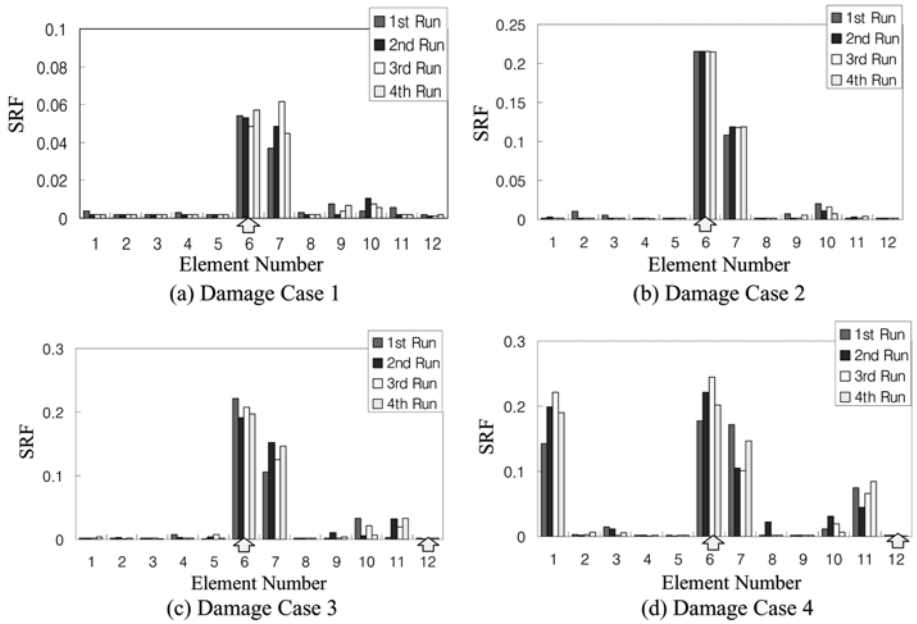

Fig. 17 Damage detection results with both frequency changes and mode-shape changes ($W_\omega = 1.0$ and $W_\phi = 0.1$)

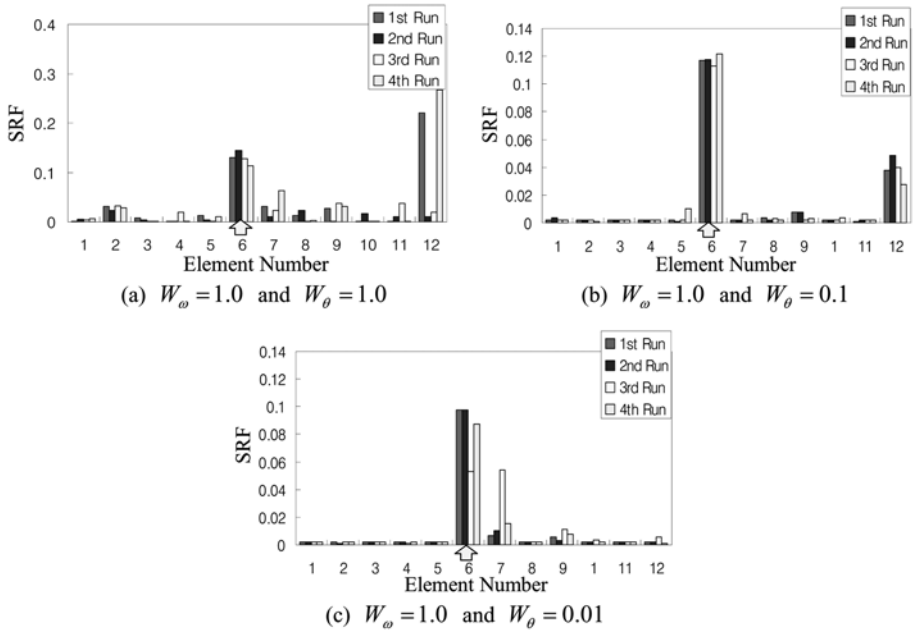

Fig. 18 Damage detection results to decide optimal weights for natural frequency and modal strain-energy (Damage Case 1)

negligible, as shown in Fig. 18(c), and the results tend to be the same as those with the frequency changes only, as shown in Fig. 13(a).

We selected the weight of 0.1 as the best weight for the modal strain-energy. With the selected

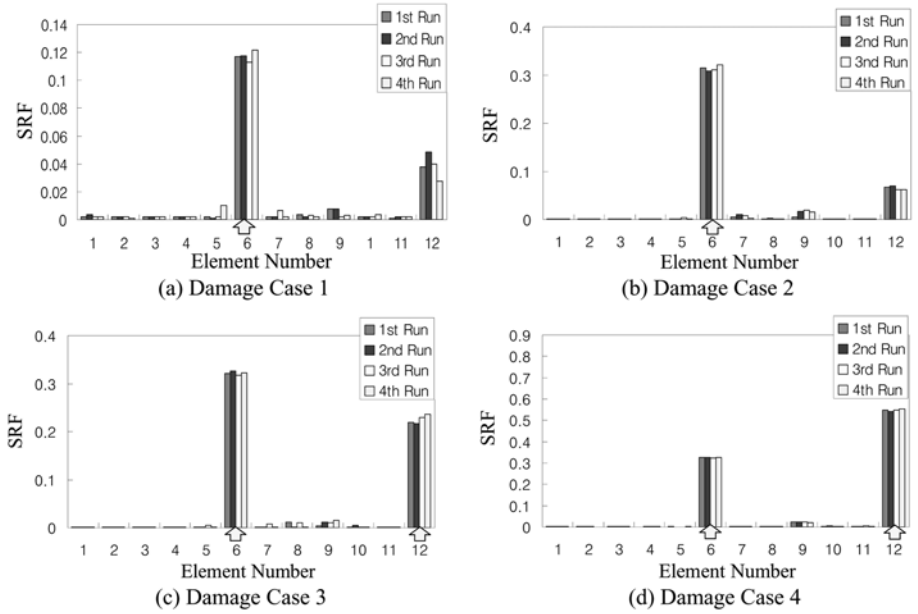

Fig. 19 Damage detection results with both frequency changes and modal strain-energy changes ($W_\omega = 1.0$ and $W_\phi = 0.1$)

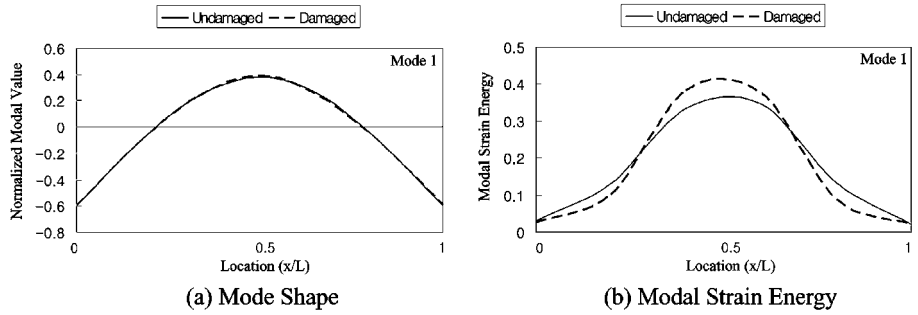

Fig. 20 Sensitivity of mode shape and modal strain energy to local damage damage Case 4

optimum weight, consistent results were predicted in subsequent four runs of GA processes. For all damage cases, Element 6 and Element 12 were detected correctly, as shown in Fig. 19. It is analyzed that the results with both the frequency changes and the modal strain-energy changes are better than those with both the frequency changes and the mode-shape changes. This may be because the modal strain-energy is more sensitive to local damages than the mode-shape. Fig. 20 illustrates the change in the first mode shape and the change in the first modal strain energy between before and after damage (e.g. Damage Case 4).

4.2. Severity estimation results of test beam

Once the damages were located, the severities of damages were also estimated from the damage detection results. Here, we limited the severity estimation to two methods: the method using both the frequency changes and the mode-shape changes (i.e. $J_1(\alpha)$ described in Eq. (10)) and the method using both frequency changes and modal strain-energy changes (i.e. $J_2(\alpha)$ described in Eq. (12)).

Table 5 Damage severity estimation results of test beam

Damage Case	Inflicted Severity		Predicted by $J_1(\alpha)$		Predicted by $J_2(\alpha)$	
	α ($x/L = 0.466$)	α ($x/L = 0.935$)	α_6	α_{12}	α_6	α_{12}
1	0.58	-	0.053	-	0.117	-
2	0.88	-	0.215	-	0.314	-
3	0.88	0.58	0.204	0	0.322	0.226
4	0.88	0.88	0.211	0	0.325	0.547

Note: α_6 = stiffness reduction factor of Element 6, α_{12} = stiffness reduction factor of Element 12

As listed in Table 3 and also described in Fig. 12, the damages were inflicted by cuts into two locations of the test beam. The damage sizes $a/t = 0.25$ and $a/t = 0.5$ approximately correspond to the fractional loss of bending stiffness 58% ($\alpha = 0.58$ and 88% ($\alpha = 0.88$, respectively, at the sections where the damages were introduced. However, the cut-induced stiffness reduction of the test structure is not identical to the element stiffness reduction of the model since the width of the cuts is not the same as the width of the element. Notice that the damage localization was performed in element scale by which we can define an element as a damage location.

Results of damage severity estimation by using the above-mentioned two methods are listed in Table 5. In Table 5, α_6 and α_{12} denote the stiffness reduction factors of Elements 6 and 12, respectively. It is observed that the method using the frequency changes and the modal strain-energy changes (i.e. $J_2(\alpha)$) shows more consistent estimation of severities than the method using the frequency changes and the mode-shape changes (i.e. $J_1(\alpha)$).

5. Concluding remarks

In this study, an improved GA-based damage detection algorithm using a set of combined modal features that include natural frequency, mode shape, and modal strain energy was proposed. In order to achieve the objective, the following approaches were implemented. Firstly, a new GA-based damage detection algorithm was formulated for beam-type structures. A schematic of the GA-based damage detection algorithm was designed and objective functions using the combined modal features are selected for the algorithm. Secondly, experimental modal tests were performed on free-free beams. Sensor locations were determined from numerical analyses. Modal features such as natural frequency, mode shape, and modal strain energy were experimentally measured before and after damaging episodes of the test beams. Finally, damage detection exercises were performed on the test beams by using the proposed GA-algorithm and the combined modal features.

We examined five potential modal features: frequency changes, mode-shape changes, modal strain-energy changes, frequency changes combined with mode-shape changes, and frequency changes combined with modal strain-energy changes. From the damage detection results, it is observed that the best modal features for the proposed technique is the frequency changes combined with the modal strain-energy changes. For the best performance of the combined objective function, the weight of natural frequency was selected as unity and the weight of modal strain-energy was selected as 0.1 (i.e. 10% relative to that of natural frequency).

Future study should be focused to determine the optimal weight for each modal feature, to rigorously verify the feasibility of the accuracy of severity estimation using the proposed method and also to evaluate the applicability of the method to other types of structures.

Acknowledgements

This study was supported by Smart Infra-Structure Technology Center (SISTeC) under the research grant (R11-2002-101-03002-0) of Korea Science and Engineering Foundation (KOSEF).

References

Au, F. T. K., Cheng, Y. S., Tham, L. G. and Bai, Z. Z. (2003), "Structural damage detection based on a micro-genetic algorithm using incomplete and noisy modal test data", *J. Sound Vib.*, **259**(5), 1081-1094.

Choi, M. Y. and Kwon, I. B. (2000), "Damage detection system of a real steel truss bridge by neural networks", *Proceedings of SPIE*, **3988**, 295-306.

Chou, J. H. and Ghaboussi, J. (2001), "Genetic algorithm in structural damage detection", *Comput. Struct.*, **79**, 1335-1353.

Friswell, M. I., Penny, J. E. T. and Garvey, S. D. (1998), "A combined genetic and eigensensitivity algorithm for the location of damage in structures", *Comput Struct.*, **69**(5), 547-556.

Goldberg, D. E. (1999), *Genetic algorithms in search, optimization & machine learning*, Addison-Wesley, New York.

Hao, H. and Xia, Y. (2002), "Vibration-based damage detection of structures by genetic algorithm", *J. Comput. Civ. Eng.*, **16**(3), 222-229.

Hoshiya, M. and Saito, E. (1984), "Structural identification by extended kalman filter", *ASCE J. Eng. Mech.*, **110**(12), 1757-1770.

Kim, J. T. (2001), "Crack detection scheme for steel plate-girder bridges via vibration-based system identification", *KSCE J. Civ. Eng.*, **5**(1), 1-10.

Kim, J. T., Ryu, Y. S., Cho, H. M. and Stubbs, N. (2003a), "Damage identification in beam-type structures: frequency-based method vs mode-shape-based method", *Eng. Struct.*, **25**(1), 57-67.

Kim, J. T. and Stubbs, N. (1995), "Model-uncertainty impact and damage detection accuracy in plate girder", *J. Struct. Eng.*, **121**(10), 1409-1417.

Kim, J. T., Yun, C. B. and Yi, J. H. (2003b), "Temperature effects on frequency-based damage detection in plate-girder bridges", *KSCE J. Civ. Eng.*, **7**(6), 725-733.

Lee, J. J. and Yun, C. B. (2006), "Two-step approaches for effective bridge health monitoring", *Struct. Eng. Mech.*, **23**(1), 75-95.

Maia, N. M. M., Silva, J. M. M. and Almas, E. A. M. (2003), "Damage detection in structures: from mode shape to frequency response function methods", *Mechanical System and Signal Processing*, **17**(3), 489-498.

Mares, C. and Surace, C. (1996), "An application of genetic algorithms to identify damage in elastic structures", *J. Sound Vib.*, **195**(2), 195-215.

Raich, A. M. and Liszkai, T. R. (2003), "Benefits of applying and implicit redundant representation genetic algorithm for structural damage detection in noisy environments", *Genetic and Evolutionary Computation Conference*, **2724**(2003), 2418-2419.

Rao, M. A., Srinivas, J. and Murthy, B. S. N. (2004), "Damage detection in vibrating bodies using genetic algorithms", *Comput. Struct.*, **82**(11/12), 963-968.

Ruotolo, R. and Surace, C. (1997), "Damage assessment of multiple cracked beams: numerical results and experimental validation", *J. Sound Vib.*, **206**(4), 567-588.

Sohn, H., Farrar, C. R., Hemez, F. M., Shucnk, D. D., Strnemates, D. W. and Nadler, B. R. (2003), "A review of structural health monitoring literature: 1996-2001", LA-13976-MS, Los Alamos National Laboratory, Los Alamos, p. 301.

Stubbs, N., Park, S., Sikorsky, C. and Choi, S. (2000), "A global non-destructive damage assessment methodology for civil engineering structures", *Int. J. System Sci.*, **42**(11), 1361-1373.

Wu, X., Ghaboussi, J. and Garrett, J. H. Jr. (1992), "Use of neural networks in detection of structural damage", *Comput. Struct.*, **42**(5), 649-659.

Yi, J. H. and Yun, C. B. (2004), "Comparative study on modal identification methods using output-only information", *Struct. Eng. Mech.*, **17**(3-4), 445-466.